Kinetic parameters for the thermal cracking of simple hydrocarbons: From laboratory to geological time-temperature conditions

V. Burklé-Vitzthum, R. Bounaceur, Raymond Michels, G. Scacchi, P.-M. Marquaire

KINETIC PARAMETERS FOR THE THERMAL CRACKING OF SIMPLE HYDROCARBONS: FROM LABORATORY TO GEOLOGICAL TIME-TEMPERATURE CONDITIONS

V. Burklé-Vitzthum [a,*], R. Bounaceur [a], R. Michels [b], G. Scacchi [a], P.-M. Marquaire [a]

[a] Laboratory of Reactions and Process Engineering, LRGP UMR 7274, CNRS, Université de Lorraine BP 20451, 54001 Nancy, France

[b] GeoRessources UMR 7359, CNRS, Université de Lorraine BP 70239, 54501 Vandœuvre-lès-Nancy, France

Corresponding author: valerie.vitzthum@univ-lorraine.fr

Abstract

Apparent kinetic parameters (frequency factor A and activation energy E_a) were computed at 700 bar and two temperatures: 200°C, a characteristic of deeply buried reservoirs of petroleum and 400°C an average temperature used for laboratory pyrolysis to simulate thermal cracking of petroleum. Several hydrocarbons were studied by simulation: several linear alkanes and one branched alkane, toluene, 2-methylnaphthalene, 1-,3-,5-trimethylbenzene, methylcyclohexane, butylcyclohexane, tetralin and decylbenzene. The calculations were performed using detailed kinetic models (mostly free-radical mechanisms) previously constructed. The computation of E_a does not depend on the global rate law, but we assumed a first-order reaction law to compute A. The apparent kinetic parameters of all hydrocarbons are slightly modified by temperature and rather strongly for tetralin and decylbenzene. The deviation, due to the use of Arrhenius law with the apparent kinetic parameters computed at 400°C for extrapolation to geological temperature, is important in most cases, even if the kinetic parameters do not strongly depend on temperature. In this study, most hydrocarbons appear more stable at 200°C than it could be inferred by using the extrapolation of the Arrhenius law from 400°C to 200°C, except for tetralin and decylbenzene which appear more reactive. The apparent kinetic parameters that were computed at 200°C could be implemented in global kinetic models used for the assessment of reservoirs.

1. Introduction

The prediction of the petroleum composition, submitted to thermal cracking over millions of years, requires a good knowledge of the reaction kinetics, particularly in deeply buried reservoirs, at high pressure (100-1000 bar) and high temperature (> 200°C). The apparent kinetic parameters (apparent frequency factor A and apparent activation energy E_a) are commonly determined via pyrolysis in laboratory at high pressure of crude oils [i.e.1-13] or pure hydrocarbons [i.e. 14-24]. The geological time is compensated by higher temperatures (350-450°C) than those encountered in reservoir. The bulk kinetic models derived from experimental results are then computed using geological time-temperature conditions. Due to the complexity of the chemical composition of crude oils, it is easier to derive reliable kinetic parameters from pyrolysis of pure hydrocarbons or simple mixtures.

In order to determine precisely the main reaction pathways and obtain reliable predictions, detailed kinetic models for the thermal reaction of pure hydrocarbons or simple mixtures can also be set up. These detailed kinetic models consist of mechanisms made of elementary steps (mainly free-radical reactions) with their fundamental kinetic parameters [25-37]. That is the reason why they can be extrapolated in the pressure and temperature ranges of 100-1000 bar and 150-450°C, respectively: the main reaction pathways and the fundamental kinetic parameters remain unchanged. The main advantages of these models are their precision and the possibility for extrapolation. However, the main drawback is the size of the model (several hundred even thousand reactions) which prevents their integration in a basin model.

This paper aims to test if the apparent kinetic parameters are constant in the temperature range of 200-400°C, at high pressure, *i.e.* testing if the apparent kinetic parameters computed at 400°C can be used at 200°C by extrapolation of the Arrhenius law in a reliable manner. A temperature equals to 200°C is typical of deeply buried oil reservoirs, and 400°C is an average temperature for laboratory pyrolysis. In this study, the selected hydrocarbons are linear and branched alkanes, several aromatic compounds (toluene, trimethylbenzene “TMB”, methylnaphthalene “MN”, decylbenzene “DB” and tetralin) and cycloalkanes (methylcyclohexane “MCH” and butylcyclohexane “BCH”). All free-radical mechanisms mentioned in this paper were constructed and validated based on experimental database recovered by our team for about 15 years ([25-28], [30-32], [34-35]). The detailed models are used to compute the apparent kinetic parameters at 700 bar and two temperatures: 200°C and

400°C. The kinetic parameters computed at 400°C and then 200°C are used to calculate and compare the conversion after 1, 10 or 100 million years at 200°C (depending on the reactivity of the compound), as well as the half-life. The relative scale of stability is set up and compared at both temperatures. This comparison is performed to highlight the influence of extrapolating kinetic parameters outside the range of temperatures in which they were computed. This work is the first step of the construction of bulk kinetic models reliable in the geological pressure and temperature conditions, and which could be implemented in complete basin models for petroleum exploration purposes.

2. Methodology for the determination of apparent kinetic parameters

Apparent kinetic parameters were first calculated at T_0 = 400°C and then 200°C, at 700 bar. The computation of the apparent activation energy does not depend on the kinetic law, when it can be done directly by the rate, but the apparent frequency factor A does. A was computed assuming that cracking reactions follow the first-order kinetic law.

The models were computed by using the package of software CHEMKIN II [38], and more precisely SENKIN at constant pressure and temperature. It should be noted that this software uses the ideal gas law to calculate concentrations. Obviously, the ideal gas law is not valid at high pressure either. Consequently, all initial concentrations c_0 were first calculated separately by using the Peng-Robinson equation of state [39] which is implemented in the software DIAGSIM [40]. The Peng-Robinson equation of state has been chosen because it is about two times more precise for the estimation of the densities than the other cubic equations of state as the Soave-Redlich-Kwong equation [41]. The calculation of the densities allows the calculation of the concentrations, and this calculation is performed to evaluate the ideal gas pressures that lead to the same initial concentrations than the Peng-Robinson equation of state computed at 700 bar. Simulation conditions are summarized in Table 1.

Simulations were performed and reached up to 30% conversion. The consumption rates r were computed by CHEMKIN at 30% conversion, and by plotting $ln\ r$ *vs* $-1/RT$ (where R is the ideal gas constant and T the temperature in K) with $T = T_0$, $T_0 - 2$, $T_0 + 2$, the slope corresponds to the apparent E_a. The first-order kinetic law ($r = k \times c$, with k the rate constant following the Arrhenius law, k in s^{-1} and c in $mol.m^{-3}$) leads to:

$$ln\ r = ln\ A - E_a/RT + ln\ c$$

The Y-intercept of the plots *ln r vs -1/RT* allows the calculation of *A*. The results are presented first at laboratory temperature (400°C) and then at geological temperature (200°C). The uncertainty on the computed apparent kinetic parameters depends on: 1) the uncertainty of the intrinsic kinetic parameters of the elementary reactions in the kinetic models, 2) the choices made during the construction of the kinetic model (detailed *vs* lumped models), 3) the care given to the computations (strict respect of the method, especially iso-conversion), and for *A*: 4) the precision of the estimation of the initial concentrations. Considering the time and effort given to the calculations, the uncertainty on apparent E_a is estimated between ± 0.5 kcal/mol and a factor of 2 for the apparent *A*.

3. Kinetic parameters at laboratory temperature (400°C)

The hydrocarbons selected for this study are divided into three groups: alkanes (linear and branched), methylaromatics (toluene, methylnaphthalene and trimethylbenzene) and other hydrocarbons, such as naphthenes (methylcyclohexane and butylcyclohexane), decylbenzene and tetralin.

3.1 Alkanes

The apparent kinetic parameters of alkanes were calculated using the detailed kinetic model of Burklé-Vitzthum et al. [30]. This model was constructed based on a lumping technique, taking into account any linear alkanes between C_1 and C_{32} as well as model compounds of branched alkanes, as reactants and any crossed reactions, and making up 13 206 free radical reactions. Alkanes with several lengths ranging from C_5 to C_{25} were studied. Linear alkanes were mostly studied, but the influence of branched structures was investigated by comparing *n*C_{15} to *iso*C_{15}.

Table 2 presents the results at 400°C. It leads to the following comments: 1) kinetic parameters of *n*- and *iso*-alkanes do not exhibit any significant differences due to their similar structure and reactivity, 2) all activation energies are comprised between 67.0±0.5 and 69.1±0.5 kcal/mol for any alkane chain length and they increase almost linearly with the chain length (Figure 1), 3) the frequency factor increases with the alkane length.

Activation energies obtained from the calculations are similar for any chain length investigated, proving the consistency of the lumping methods results with those of detailed

mechanisms. A mean value of 68.5 kcal/mol could be proposed, for every alkane for any structure and length (n> 4).

For nC$_8$, the detailed model (91 free radical reactions) of Lannuzel et al. [33] was also tested, and leads to $A = 6.5\times10^{16}$ s^{-1} and E_a = 67.6 kcal/mol, as well as the extended model of Bounaceur et al. [26] (182 free radical reactions) which leads to $A = 6.6\times10^{15}$ s^{-1} and E_a = 64.0 kcal/mol. The very simple model of Burklé-Vitzthum et al. [29] in the case of nC$_{16}$ (13 free radical reactions), which was constructed using a particularly drastic lumping method, leads to $A = 2.0\times10^{15}$ s^{-1} and E_a = 61.8 kcal/mol.

The former mechanisms were all constructed and validated at high pressure (700 bar) and temperatures in the range of 300 - 400°C.

Another detailed model [42] was also tested: it was constructed to describe the cracking of nC$_{12}$ in jet fuel conditions (typically 1 bar and 800°C). In these conditions, short radicals formed via decompositions are predominant, whereas in our conditions (lower temperature and very high pressure), the predominant radicals are those corresponding to the reactant, which are formed via H-transfers [26]. Indeed high pressures favor bimolecular reactions, on the contrary to low pressures that favor unimolecular reactions. Therefore, the free radical reactions, that determine the cracking rates, are different and consequently the apparent kinetic parameters are totally different, even when the mechanism is computed at 400°C and 700 bar: $A = 4.5\times10^{13}$ s^{-1} and E_a = 55.9 kcal/mol ($A = 1.6\times10^{12}$ s^{-1} and E_a = 50.4 kcal/mol when the mechanism is computed at P = 1 bar and T = 800°C). This example illustrates the importance of selecting kinetic parameters that are determined in conditions close to those in which they are used.

Table 3 gathers the experimental literature data concerning *n*-alkanes in similar T and P conditions, but the results appear very scattered: $59 < E_a < 74$ kcal/mol and $3\times10^{13} < A < 7\times10^{22}$ s^{-1}. The activation energy seems to increase with pressure, but no clear conclusion can be drawn. Agreement is obtained with Béhar and Vandenbroucke [14] and Khorasheh and Gray [20] for nC$_{16}$ lumped in a drastic manner, and our results are consistent with those of Song et al. [46] and Zhou and Crynes [45].

3.2 Methylaromatics

Three methylaromatics were studied: toluene [32], 1-methylnaphthalene [35] and 1, 3, 5-trimethylbenzene [31]. Table 2 gathers the results obtained via computation of the models. The apparent activation energies of the studied methylaromatics are very close, due to their similar structures. The apparent frequency factor of trimethylbenzene is higher than that of toluene due to the reaction path degeneracy.

Literature data concerning several aromatics is presented in Table 3. Some data was found at the same *P-T* conditions. Concerning toluene, literature activation energies are much higher than those calculated from our mechanisms, but they were determined at higher temperatures and at atmospheric pressure. In these conditions, the cracking mechanisms are different [32]; particularly the bimolecular initiations are negligible while they are of utmost importance at high pressures. Indeed, activation energies of bimolecular initiations are 30 kcal/mol lower than unimolecular ones, but they become important only at high pressure and therefore the apparent activation energy is much lower at high pressure than at low pressure. Agreement between experimental [31] and computed activation energy of trimethylbenzene is obtained. Concerning 1-methylnaphthalene, the experimental activation energy [24] is far lower than the computed value. The determination of the experimental apparent activation energy requires the determination or the assumption of the kinetic law, which is not needed for the computation of E_a by our kinetic model using detailed mechanisms (the software CHEMKIN II computes directly the rates according to the reaction mechanisms implied). The determination of the experimental E_a is generally performed by assuming a first-order law but we demonstrated elsewhere [35] that this assumption is not always true. This may explain the differences between the experimental apparent activation energy and the computed value, especially for methylnaphthalene.

3.3 Other hydrocarbons

Methylcyclohexane [27], butylcyclohexane [34], decylbenzene [28] and tetralin [25] were also studied. The apparent kinetic parameters are in Table 2. The apparent activation energies are in the same order of magnitude at 400°C. Butylcyclohexane appears more reactive than methylcyclohexane. This is due to the cracking of the butyl side chain which is easier than the cracking of the methyl side chain. The literature data concerning naphthenes are presented in Table 3. No literature data was found for methylcyclohexane, but the computed kinetic

parameters of butycyclohexane are very close to the experimental ones determined for butycyclohexane [52, 53] and propylcyclohexane [54].

The computed results of tetralin are far from the values obtained by Yu and Eser [55], although they were determined in neighboring conditions. This difference can be due to the assumption of a first-order kinetic law to determine the experimental value. According to our model, it appears that this assumption is not justified [25]. Another sensitive factor is the amount of impurities [25] (particularly dihydronaphthalene) which greatly influences the reactivity of tetralin and consequently its apparent kinetic parameters. This point is not clearly addressed in the experimental study by Yu and Eser [54] and so the comparison is difficult. In our case, the computations were performed with 0.1% of dihydronaphthalene. The mechanism of 2-ethyltetralin is strongly influenced by the cracking of the side chain and so the comparison with tetralin would not be consistent.

Concerning long-chain ($n \geq 4$) alkylbenzene in which the long chain allows the retroene reaction [28], no agreement is obtained with the literature data, except with the activation energy of Leigh and Szwarc [50] and the frequency factor of Yu and Eser. These results are surprising but once again, literature data were generally determined at higher temperatures and much lower pressures than in our study, making comparisons quite difficult.

3.4 Relative thermal stability at 400°C

To establish a relative scale of stability of the investigated hydrocarbons at 400°C, the conversion X is plotted as a function of temperature T assuming a first-order reaction law (Figure 2). The pyrolysis duration is set to 10 hours, which is a typical duration for pyrolysis in the laboratory. Characteristic S-shaped curves are obtained (Figure 2). The scale of stability between compounds is determined as following: the higher the temperature to reach 50% conversion, the more stable the compound. The following scale is obtained from the least to the most stable compound:

DB < C_{15} < MN < BCH < Tetralin < MCH ≈ TMB < toluene

It should be noted that: 1) long alkanes (C_{15}) belong to compounds with low stability, 2) cycloalkanes are more stable than C_{15}, 3) toluene and trimethylbenzene are the most stable compounds and behave very differently from methylnaphthalene and decylbenzene, 4)

alkylbenzenes are increasingly reactive as their side chain length increases, 5) the stability of the aromatic compounds strongly depends on their structure.

The relative stability of butylcyclohexane and alkanes was studied elsewhere [34] and the relative scale of stability was:

$nC_{25} < nC_{16} < nC_{10} \approx BCH < nC_8$

This is in agreement with our results.

The relative stability of dodecylbenzene, 9-methylphenanthrene and nC$_{25}$ was evaluated by Béhar et al. (2008), and it should be noted that our results concerning decylbenzene (instead of dodecylbenzene), methylnaphthalene (instead of 9-methylphenanthrene) and nC$_{15}$ (instead of nC$_{25}$) are in agreement with their results at 400°C.

4. Kinetic parameters at geological temperature (200°C)

4.1 Alkanes and methylaromatics

Alkanes and methylaromatics kinetic parameters seem to be almost constant between 400°C and 200°C (Table 2) because the free-radical reactions that control the thermal cracking remain the same. The apparent activation energy of alkanes does not depend on the chain length at 200°C on the contrary to 400°C and an average value of 69.3±0.5 kcal/mol can be proposed for any chain length. Nevertheless, the apparent rate constant k increases with the chain length and its evolution can be compared to the correlation of Watanabe et al. [56] validated at 200-700°C and 1-150 bar. Watanabe et al. [56] proposed a correlation that plots $k(nC_i)/k(nC_{16})$ as a function of the chain length i ($3 \leq i \leq 32$) regardless of the temperature and the pressure. The correlation was validated up to $i \approx 20$. We have chosen arbitrarily C$_{15}$ as a reference alkane instead of C$_{16}$ in this study, so we plotted $k(nC_i)/k(nC_{15})$ [26, 29, 30, 33] at 400°C and 200°C as a function of i and we compared it to the correlation established for $k(nC_i)/k(nC_{16})$ (Figure 3). Agreement with the model [56] was obtained at up to i = 16 for both temperatures.

4.2 Other hydrocarbons

Table 2 shows that the behavior of decylbenzene and tetralin strongly depends on temperature. In the case of decylbenzene, the previous mechanistic study [28] revealed that the mechanism includes free-radical reactions as well as the molecular retroene reaction. The

236 importance of the retroene reaction increases as temperature decreases because its activation
237 energy (54 kcal/mol) is much lower than the global cracking activation energy of the free-
238 radical (70 kcal/mol). Indeed, at low temperature, the apparent activation energy almost
239 corresponds to the activation energy of the retroene reaction.

240 The apparent activation energy of tetralin strongly decreases when the temperature decreases
241 but so does the frequency factor. This is due to the bimolecular initiations whose kinetic
242 parameters are much lower than those of unimolecular initiations. So their importance
243 increases when temperature decreases and they strongly influence the apparent kinetic
244 parameters, leading to lower frequency factors and lower activation energies.

245 *4.3 Relative thermal stability at 200°C*

246 A relative scale of stability is established at 200°C in the same manner as previously for
247 400°C, but the duration is set to 100 million years (Figure 4) which is characteristic of
248 geological duration. The apparent kinetic parameters computed at 200°C are used. A different
249 scale of stability is obtained at 200°C (Figure 4) in comparison to 400°C (Figure 2),
250 essentially because the apparent activation energies are different for each compound, but also
251 because of the modification of some kinetic parameters with temperature:

252 DB < MN < C_{15} ≈ TMB < tetralin ≈ BCH ≈ toluene < MCH

253 One major difference between both scales of stability is the increase of the relative stability of
254 methylcyclohexane when temperature decreases. Another major difference is the strong
255 increase of the reactivity of decylbenzene with the decrease of temperature due to the retroene
256 reaction as explained above.

257 The comparison between the relative scales of stability at low and high temperatures appears
258 more difficult for the other compounds. In order to highlight the influence of the
259 modifications of the apparent kinetic parameters, we also computed the relative scale of
260 stability at 200°C, but with the kinetic parameters computed at 400°C, and we obtained:

261 DB ≈ MN < TMB < C_{15} < toluene < BCH ≈ MCH≈ tetralin

262 The major mistake that would be done by using at 200°C the kinetic parameters computed at
263 400°C, would lie in the overestimation of the stability of tetralin and decylbenzene, in
264 comparison to the other compounds.

5. Discussion

The apparent kinetic parameters of decylbenzene, methylcyclohexane and tetralin clearly depend on temperature. For all other compounds, the differences between the kinetic parameters computed at 400°C and 200°C could seem negligible. In order to quantify the consequences of these minor changes, we calculated the conversion at 200°C after 1, 10 or 100 million years (depending on the reactivity of the hydrocarbon) by using the apparent kinetic parameters computed at 400°C and 200°C and assuming a first-order law (Table 4). We also calculated the half-life with both apparent kinetic parameters (Figures 5, 6 and 7).

5.1. Alkanes

Table 4 and Figure 5 show that simulating at 200°C the apparent kinetic parameters computed at 400°C would lead to a higher reactivity (increase of conversion and decrease of half-life) than using the kinetic parameters computed at 200°C, especially for short alkanes (nC$_8$). The difference is less important when the length of alkanes increases and there is no difference for long alkanes (nC$_{25}$).

Differences could be explained by on the weight of decomposition reactions via β-scission of the short radicals among all decomposition reactions. Indeed, the decomposition reactions are rate-limiting at high pressures and low temperatures [26] and they greatly influence the apparent activation energy. The kinetic parameters of the decomposition of short radicals depend more on temperature (higher activation energy) than the kinetic parameters of the other radicals [26]. Moreover, for short alkanes, the weight of decomposition of short radicals among all decomposition reactions is more important than for long-chain alkanes: short radicals are more concentrated during the thermal cracking of short alkanes than of long alkanes. That is why the apparent activation energy of short alkanes depends more on temperature than that of long alkanes. As a consequence, the errors made when simulating at 200°C the kinetic parameters determined at 400°C lies on the fact that the alkane studied is short.

5.2. Monoaromatics and naphthenes

The computed conversions and half-lives are presented in Table 4, and Figure 6. All these compounds appear to be more stable at 200°C than at 400°C. With the apparent kinetic parameters computed, the conversions are lower while the half-lives higher at 200°C than at

400°C, although the apparent kinetic parameters do not seem to depend on temperature except for methylcyclohexane. In order to evaluate more precisely the temperature-dependence of the apparent first-order kinetic constant k of methylcyclohexane, we computed *k(T)* in the temperature range of 200-400°C and we plotted *k(T) vs 1/RT* (R: ideal gas constant and T: temperature) in a logarithmic scale (markers in Figure 8). By considering the apparent kinetic parameters (A and E_a) computed at 400°C, we extrapolated the Arrhenius law from 400°C to low temperature and the extrapolated rate constant is referred to *k(400)*. Then we plotted *k(400) vs 1/RT* (straight lines in a logarithmic scale in Figure 8). It clearly appears that the deviation between *k(400)* and *k(T)* increases when the temperature decreases and that *k(T) < k(400)*.

5.3. Decylbenzene and tetralin

The computed conversions and half-lives are presented in Table 4 and Figure 7. Unlike the other hydrocarbons studied, decylbenzene and tetralin appear to be more reactive at 200°C than at 400°C. When the apparent kinetic parameters are computed at 200°C the conversions are higher and the half-lives lower than at 400°C. In the case of decylbenzene, as explained above, this increasing reactivity is due to the retroene reaction whose activation energy is particularly low and whose importance increases when the temperature decreases [28]. The increasing reactivity of tetralin is probably related to the bimolecular initiations whose importance also increases when the temperature decreases because of their lower activation energy than that of unimolecular initiations [25].

The apparent kinetic parameters of decylbenzene and tetralin (Table 2) strongly depend on temperature. In order to evaluate precisely the temperature-dependence of the apparent first-order kinetic constant k of decylbenzene and tetralin, we computed *k(T)* in the temperature range of 200-400°C and we plotted *ln k(T) vs 1/RT* as well as *ln k(400) vs 1/RT* (Figure 8). It also clearly appears that the deviation between *k(400)* and *k(T)* increases when the temperature decreases and that *k(T) > k(400)*.

6. Conclusion

In this paper we computed the apparent kinetic parameters (frequency factor A and activation energy E_a) of several pure hydrocarbons on the basis of detailed kinetic models previously constructed and validated. The purpose was to evaluate the effects of extrapolating data obtained in a range of temperatures to another. Indeed, thermal cracking reactions take place

326 at 150°C - 200°C for millions of years in geological reservoirs and so all laboratory data are
327 obtained at about 400°C during some hours or days and then extrapolated.

328 The calculations were performed at 700 bar and at 400°C and then 200°C. The computation of
329 E_a is independent from the kinetic rate law with our method, but the computation of A is not:
330 we postulated a first-order kinetic law which is of use in the vast majority of geochemistry
331 publications. In the present study, most of the compounds exhibit apparent kinetic parameters
332 that are slightly or even highly different between 400°C and 200°C. Extrapolating apparent
333 kinetic parameters obtained at 400°C, even though they are only slightly different from those
334 at 200°C, can lead to significant differences in terms of half-lives or conversion after several
335 millions of years. All hydrocarbons studied here (alkanes, monoaromatics and naphthenes)
336 appear to be more stable at 200°C than when extrapolating the Arrhenius law from 400°C to
337 200°C, except decylbenzene and tetralin which appear much more reactive. To conclude, any
338 extrapolation beyond the original range of temperatures used to determine the apparent kinetic
339 parameters has to be considered very carefully, in the geochemistry field, but also in any other
340 application fields of thermal cracking. We previously showed [26] that the same is true for the
341 extrapolation beyond the original range of pressure because the importance of bimolecular vs
342 unimolecular reactions can be completely modified.

343 To complete the discussion, two more points should be addressed: the choice of the kinetic
344 rate law and the effects of co-reactants. In most studies, a first-order kinetic law is postulated,
345 although it clearly appears that this choice is erroneous for some compounds; for instance, the
346 order is close to ½ for pure alkanes [57] and 2 for pure methylnaphthalene [35]. It would be
347 interesting to lead a complete study on the best choice of kinetic order for each hydrocarbon
348 and address the consequences of an erroneous choice on hydrocarbon stability. The second
349 point is the effects of co-reactants on the apparent kinetic parameters. We showed on several
350 systems ([29, 33, 58, 59]) that some co-reactants can completely change the stability of
351 hydrocarbons and consequently the apparent kinetic parameters are also very likely to be
352 modified. ~~Therefore, the studies on pure hydrocarbons have a limited range of application.~~ In
353 order to construct bulk kinetic models of mixtures meant to represent oil fractions, a similar
354 study as the one presented here should be performed with binary mixtures: correlations
355 between the apparent kinetic parameters and the content of co-reactants could be obtained and
356 then used in bulk kinetic models.

357

References

[1] P. Ungerer, R. Pelet, Extrapolation of the kinetics of oil and gas formation from laboratory experiments to sedimentary basins, Nature 327 (1987) 52-54.

[2] P. Ungerer, F. Béhar, M. Villalba, O.R. Heum, A. Audibert, Kinetic modelling of oil cracking, Org. Geochem. 13 (1988) 857-868.

[3] F. Béhar, S. Kressmann, J.L. Rudkiewicz, M. Vandenbroucke, Experimental simulation in a confined system and kinetic modelling of kerogen and oil cracking, Org. Geochem. 19 (1992) 173–189.

[4] F. Béhar, Y. Tang, J. Liu, Comparison of rate constants for some molecular tracers generated during artificial maturation of kerogens: influence of kerogen type, Org. Geochem. 26 (1997) 281–287.

[5] F. Béhar, M. Vandenbroucke, Y. Tang, F. Marquis, J. Espitalié, Thermal cracking of kerogen in open and closed systems: determination of kinetic parameters and stoichiometric coefficients for oil and gas generation, Org. Geochem. 26 (1997) 321–339.

[6] F. Béhar, F. Lorant, L. Mazeas, Elaboration of a new compositional kinetic schema for oil cracking, Org. Geochem. 39 (2008) 764-782.

[7] H.J. Schenk, R. Di Primio, B. Horsfield, The conversion of oil into gas in petroleum reservoirs. Part 1: Comparative kinetic investigation of gas generation from crude oils of lacustrine, marine and fluviodeltaic origin by programmed-temperature closed-system pyrolysis, Org. Geochem. 26 (1997) 467–481.

[8] V. Dieckmann, H.J. Schenk, B. Horsfield, D.H. Welte, Kinetics of petroleum generation and cracking by programmed-temperature closed-system pyrolysis of Toarcian Shales, Fuel 77 (1998) 23-31.

[9] M.D. Lewan, T.E. Ruble, Comparison of petroleum generation kinetics by isothermal hydrous and nonisothermal open-system pyrolysis, Org. Geochem. 33 (2002) 1457-1475.

[10] M.D. Lewan, M.J. Kotarba, J.B. Curtis, D. Wieclaw, P. Kosakowski, Oil-generation kinetics for organic facies with Type-II and -IIS kerogen in the Menilite Shales of the Polish Carpathians, Geochim. Cosmochim. Acta 70 (2002) 3351-3368.

386 [11] E. Lehne, V. Dieckmann, Bulk kinetic parameters and structural moieties of asphaltenes
387 and kerogens from a sulphur-rich source rock sequence and related petroleums, Org.
388 Geochem. 38 (1997) 1657-1679.

389 [12] E. Lehne, V. Dieckmann, The significance of kinetic parameters and structural markers
390 in source rock asphaltenes, reservoir asphaltenes and related source rock kerogens, the
391 Duvernay Formation (WCSB), Fuel 86 (2007) 887-901.

392 [13] F. Béhar, H. Budzinski, M. Vandenbroucke, Y. Tang, Methane Generation from Oil
393 Cracking: Kinetics of 9-Methylphenanthrene Cracking and Comparison with Other Pure
394 Compounds and Oil Fractions, Energy Fuels 13 (1999) 471-481.

395 [14] F. Béhar, M. Vandenbroucke, Experimental Determination of the Rate Constants of the
396 n-C25 Thermal Cracking at 120, 400, and 800 bar: Implications for High-Pressure/High-
397 Temperature Prospects, Energy Fuels 10 (1996) 932-940.

398 [15] K.J. Jackson, A.K. Burnham, R.L. Braun, K.G. Knauss, Temperature and pressure
399 dependence of n-hexadecane cracking, Org. Geochem. 23 (1995) 941–953.

400 [16] F. Enguehard, S. Kressmann, F. Dominé, Kinetics of dibutylether pyrolysis at high
401 pressure – experimental study, Org. Geochem. 16 (1990) 155-160.

402 [17] F. Béhar, F. Lorant, H. Budzinski, E. Desavis, Thermal Stability of Alkylaromatics in
403 Natural Systems: Kinetics of Thermal Decomposition of Dodecylbenzene, Energy Fuels 16
404 (2002) 831-841.

405 [18] C. Dartiguelongue, F. Béhar, H. Budzinski, G. Scacchi, P-M. Marquaire, Thermal
406 stability of dibenzothiophene in closed system pyrolysis: Experimental study and kinetic
407 modeling, Org. Geochem. 37 (2006) 98-116.

408 [19] T. Ford, Liquid-Phase Thermal Decomposition of Hexadecane: Reaction Mechanisms,
409 Ind Eng. Chem. Fundam. 25 (1986) 240-243.

410 [20] F. Khorasheh, M. R. Gray, High-Pressure Thermal Cracking of n-Hexadecane, Ind. Eng.
411 Chem. Res. 32 (1993) 1853-1863.

412 [21] P.E. Savage, M.T. Klein, Asphaltene Reaction Pathways. 2. Pyrolysis of n-
413 Pentadecylbenzene, Ind. Eng. Chem. Res. 26 (1987) 488-494.

414 [22] P.E. Savage, M.T. Klein, Asphaltene Reaction Pathways. 4. Pyrolysis of
415 Tridecylcyclohexane and 2-Ethyltetralin, Ind. Eng. Chem. Res. 27 (1988) 1348-1356.

[23] P.E. Savage, K.L. Baxter, Pathways, Kinetics, and Mechanisms for 2-Dodecyl-9,10-dihydrophenanthrene Pyrolysis, Ind. Eng. Chem. Res. 35 (1996) 1517-1523.

[24] J-P. Leininger, F. Lorant, C. Minot, F. Béhar, Mechanisms of 1-methylnaphthalene pyrolysis in a batch reactor, Energy Fuels 20 (2006) 2518-2530.

[25] R. Bounaceur, G. Scacchi, P-M. Marquaire, F. Dominé, Mechanistic modeling of the thermal cracking of tetralin, Ind. Eng. Chem. Res. 39 (2000) 4152-4165.

[26] R. Bounaceur, F. Lannuzel, R. Michels, G. Scacchi, P-M. Marquaire, V. Burklé-Vitzthum, Influence of pressure (100 Pa-100 MPa) on the pyrolysis of an alkane at moderate temperature (603K-723 K): Experiment and kinetic modeling, J. Anal. Appl. Pyrolysis 122 (2016) 442-451.

[27] R. Bounaceur, V. Burklé-Vitzthum, P-M. Marquaire, L. Fusetti, Mechanistic modeling of the thermal cracking of methylcyclohexane near atmospheric pressure, from 250 to 1000°C, Identification of aromatization pathways, J. Anal. Appl. Pyrolysis 103 (2013) 240-254.

[28] V. Burklé-Vitzthum, R. Michels, G. Scacchi, P-M. Marquaire, Mechanistic Modeling of the Thermal Cracking of Decylbenzene, Ind. Eng. Chem. Res. 23 (2003) 5791-5808.

[29] V. Burklé-Vitzthum, R. Michels, G. Scacchi, P-M. Marquaire, D. Dessort, B. Pradier, O. Brevart, Kinetic Effect of Alkylaromatics on the Thermal Stability of Hydrocarbons under Geological Temperatures, Org. Geochem. 35 (2004) 3-31.

[30] V. Burklé-Vitzthum, R. Bounaceur, P-M. Marquaire, F. Montel, L. Fusetti, Thermal evolution of n- and iso-alkanes in oils. Part 1: Pyrolysis model for a mixture of 78 alkanes (C1-C32) including 13,206 free radical reactions, Org. Geochem. 42 (2011) 439-450.

[31] L. Fusetti, F. Béhar, R. Bounaceur, P-M. Marquaire, K. Grice, S. Derenne, New insights into secondary gas generation from the thermal cracking of oil: Methylated aromatics. A kinetic approach using 1,2,4-trimethylbenzene. Part I: A mechanistic model, Org. Geochem. 41 (2010) 146-167.

[32] F. Lannuzel, R. Bounaceur, R. Michels, G. Scacchi, P-M. Marquaire, An extended mechanism including high pressure conditions (700 bar) for toluene pyrolysis, J. Anal. Appl. Pyrolysis 87 (2010) 236-247.

[33] F. Lannuzel, R. Bounaceur, R. Michels, G. Scacchi, P-M. Marquaire, Reassessment of the kinetic influence of toluene on *n*-alkane pyrolysis, Energy Fuels 24 (2010) 3817-3830.

[34] D. Rakatoalimanana, F. Béhar, R. Bounaceur, V. Burkle-Vitzthum, P-M. Marquaire, Thermal cracking of n-butylcyclohexane at high pressure (100 bar) – part 2: mechanistic modeling, J. Anal. Appl. Pyrolysis, 120 (2016) 174-185.

[35] R. Bounaceur, J.F. Leininger, F. Lorant, P-M. Marquaire, V. Burklé-Vitzthum, Kinetic modeling of 1-Methylnaphthalene pyrolysis at high pressure (100 bar), J. Anal. Appl. Pyrolysis (2017) accepted JAAP3952.

[36] F. Dominé, P.M. Marquaire, C. Muller, G.M. Côme, Kinetics of hexane pyrolysis at very high pressures. 2. Computer modeling, Energy Fuels 4 (1990) 2-10.

[37] F. Dominé, R. Bounaceur, G. Scacchi, P.M. Marquaire, D. Dessort, B. Pradier, O. Brevart, Up to what temperature is petroleum stable? New insights from a 5200 free radical reactions model, Org. Geochem. 33 (2002) 1487–1499.

[38] R.J. Kee, F.M. Rupley, J.A. Miller, Chemkin-II: A Fortran chemical kinetics package for the analysis of gas-phase chemical kinetics. Sandia National Laboratories, Livermore, CA, 1989.

[39] D.-Y Peng, D. B. Robinson, A new two-constant equation of state, Ind. Eng. Chem. Fundam. 15 (1976) 59-64.

[40] J-N. Jaubert, Présentation du logiciel DiagSim permettant de faciliter l'enseignement de la thermodynamique technique, International Journal of Technologies in Higher Education 2 (2005) 34-47.

[41] R. Privat, M. Visconte, A. Zazoua-Khames, J-N. Jaubert, R. Gani, Analysis and prediction of the alpha-function parameters used in cubic equations of state, Chem. Eng. Sc. 126 (2015) 584-603.

[42] O. Herbinet, P-M. Marquaire, F. Battin-Leclerc, R. Fournet, Thermal stability of n-dodecane: experiments and kinetic modeling, J. Anal. Appl. Pyrolysis 78 (2007) 419-429.

[43] D. Kunzru, Y. T. Shah, E. B. Stuart, Thermal Cracking of n-Nonane, Ind. Eng. Chem. Process Des. Dev. 11 (1972) 605-612.

[44] J. Yu, S. Eser, Kinetics of Supercritical-Phase Thermal Decomposition of C10-C14

Normal Alkanes and Their Mixtures, Ind. Eng. Chem. Res. 36 (1997) 585-591.

[45] P. Zhou, B.L. Crynes, Thermolytic Reactions of Dodecane. Ind.Eng. Chem. Process Des. Dev. 25 (1986) 508-514.

[46] C. Song, W.C. Lai, H.H. Schobert, Condensed-Phase Pyrolysis of n-Tetradecane at Elevated Pressures for Long Duration. Product Distribution and Reaction Mechanisms, Ind. Eng. Chem. Res. 33 (1994) 534-547.

[47] B. Blouri, F. Hamdan, D. Herault, Mild Cracking of High-Molecular-Weight Hydrocarbons, Ind. Eng. Chem. Process Des. Dev. 24 (1985) 30-37.

[48] S.B. Domke, R.F. Pogue, F.J.R. Van Neer, C.M. Smith, Investigation of the kinetics of ethylbenzene pyrolysis using a temperature-scanning reactor, Ind. Eng. Chem. Res. 40 (2001) 5878-5884.

[49] W.D. Clark, S.P. Price, Free-radical and MolecularProcesses in the Pyrolysis of Ethylbenzene, Can. J. Chem. 48 (1970) 1059.

[50] C.H. Leigh, M. Szwarc, The pyrolysis of normal-butylbenzene and the heat of formation of normal-propyl radical, J. Chem. Phys. 20 (1952) 407-411.

[51] H. Freund, W.N. Olmstead, Detailed chemical kinetic modeling of butylbenzene pyrolysis, Int. J. Chem. Kinet. 21 (1989) 561-574.

[52] J. Yu, S. Eser, Thermal Decomposition of Jet Fuel Model Compounds under Near-Critical and Supercritical Conditions. 1. n-Butylbenzene and n-Butylcyclohexane, Ind. Eng. Chem. Res. 37 (1998) 4591-4600.

[53] D. Rakatoalimanana, F. Béhar, R. Bounaceur, V. Burklé-Vitzthum, P-M. Marquaire, Thermal cracking of n-butylcyclohexane at high pressure (100 bar) – part 1: experimental study, J. Anal. Appl. Pyrolysis, 117 (2016) 1-16.

[54] J. A. Widegren, T. J. Thomas, Thermal decomposition kinetics of kerosene-based rocket propellants. 1. Comparison of RP-1 and RP-2, Energy Fuels 23 (2009) 5517-5522.

[55] J. Yu, S. Eser, Thermal Decomposition of Jet Fuel Model Compounds under Near-Critical and Supercritical Conditions. 2. Decalin and Tetralin, Ind. Eng. Chem. Res. 37 (1998) 4601-4608.

501 [56] M. Watanabe, T. Adschiri, K. Arai, Overall Rate Constant of Pyrolysis of n-Alkanes at a
502 Low Conversion Level, Ind. Eng. Chem. Res. 40 (2001) 2027-2036.

503 [57] R. Bounaceur, Modélisation cinétique de l'évolution thermique des pétroles dans les
504 gisements, PhD Thesis, INPL Nancy France, 2001.

505 [58] V. Burklé-Vitzthum, R. Michels, R. Bounaceur, P-M. Marquaire, G. Scacchi,
506 Experimental study and modelling of the role of hydronaphthalenics on the thermal stability
507 of hydrocarbons under laboratory and geological conditions, Ind. Eng. Chem. Res. 44 (2005)
508 8972-8987.

509 [59] R. Bounaceur, G. Scacchi, P-M. Marquaire, F. Dominé, O. Brévart, D. Dessort, B.
510 Pradier, Inhibiting effect of tetralin on the pyrolysic decomposition of hexadecane.
511 Comparison with toluene, Ind. Eng. Chem. Res. 41 (2002) 4689-4701.

512

513 **List of tables**

514 Table 1: Simulation conditions deduced from Peng Robinson equation of state.

	Initial concentration (mol/m^3) 700 bar - 400°C	**Ideal gas pressure (bar) equivalent to 700 bar at 400°C**	**Initial concentration (mol/m^3) 700 bar - 200°C**	**Ideal gas pressure (bar) equivalent to 700 bar at 200°C**
***n*C_5H_{12}**	6948	389	8319	327
***n*C_6H_{14}**	6280	351	7330	288
***n*C_8H_{18}**	5208	291	5878	231
***n*$C_{12}H_{26}$**	3602	202	3903	153
***n*$C_{14}H_{30}$**	3038	170	3250	128
***n*- or *iso* $C_{15}H_{32}$**	2797	156	2976	117
***n*$C_{16}H_{34}$**	2579	144	2731	107
***n*$C_{25}H_{52}$**	1376	77	1420	56
Toluene	7470	418	8700	342
1-Methyl-naphtalene	5919	331	6494	255
Trimethyl-benzene	6002	336	6756	266
Decylbenzene	3080	172	3281	129
Tetralin	5793	324	6404	252
Methyl-cyclohexane	6526	365	7486	294
Butylcyclohexane	4744	265	5223	205

515

516

517

518

519

520

521 Table 2: Computed apparent kinetic parameters.

522

Hydrocarbons	A (s^{-1})	E_a (kcal/mol)	A (s^{-1})	E_a (kcal/mol)
	400°C		200°C	
***n*C$_5$H$_{12}$ [30]**	1.1×10^{16}	67.2	5.3×10^{16}	69.2
***n*C$_6$H$_{14}$ [30]**	3.6×10^{16}	67.3	1.6×10^{17}	69.3
***n*C$_8$H$_{18}$ [30]**	7.7×10^{16}	67.0	1.8×10^{17}	69.2
***n*C$_8$H$_{18}$ [26]**	6.6×10^{15}	64.0	1.7×10^{18}	71.8
***n*C$_8$H$_{18}$ [33]**	6.5×10^{16}	67.6		
***n*C$_{12}$H$_{26}$ [30]**	1.8×10^{17}	68.6	2.2×10^{17}	69.3
***n*C$_{14}$H$_{30}$ [30]**	1.6×10^{17}	68.2	3.0×10^{17}	69.2
***n*C$_{15}$H$_{32}$ [30]**	1.8×10^{17}	67.8	5.2×10^{17}	69.3
***iso*C$_{15}$H$_{32}$ [30]**	1.7×10^{17}	67.9	5.3×10^{17}	69.3
***n*C$_{16}$H$_{34}$ [29]**	2.0×10^{15}	61.8		
***n*C$_{25}$H$_{52}$ [30]**	6.5×10^{17}	69.1	7.3×10^{17}	69.2
Toluene	2.9×10^{10}	54.4	4.0×10^{10}	55.4
1-Methylnaphtalene	1.3×10^{14}	59.3	1.8×10^{14}	60.2
Trimethylbenzene	8.8×10^{11}	56.1	1.4×10^{12}	57.3
Decylbenzene	1.2×10^{18}	67.0	4.9×10^{12}	54.0
Tetralin	7.4×10^{15}	67.5	2.6×10^{13}	61.2
Methylcyclohexane	1.9×10^{14}	63.7	1.5×10^{15}	66.4
Butylcyclohexane	4.7×10^{16}	68.4	7.6×10^{16}	69.4

523

524

525

526

527 Table 3: Literature data.

528

Compound	**E (kcal/mol)**	**A (s^{-1})**	**Ref.**	**T-P conditions**
***n*C$_9$H$_{20}$**	63	2.0×10^{14}	Kunzru et al., [42]	650-750°C
***n*C$_{10}$H$_{22}$**	60	3.6×10^{21}	Yu and Eser, [43]	400-450°C 21 bar
***n*C$_{12}$H$_{26}$**	62	2.3×10^{22}	Yu and Eser, [43]	400-450°C 18 bar
***n*C$_{12}$H$_{26}$**	65.2	3.7×10^{16}	Zhou and Crynes, [44]	250-440°C 92-103 bar
***n*C$_{14}$H$_{30}$**	63	7.2×10^{22}	Yu and Eser, [43]	400-450°C 16 bar
***n*C$_{14}$H$_{30}$**	67.6	7.2×10^{18}	Song et al., [45]	450°C 20-90 bar
***n*C$_{16}$H$_{34}$**	59.2	3.1×10^{13}	Blouri et al., [46]	350-440°C 20 bar
***n*C$_{16}$H$_{34}$**	59.6	3.1×10^{14}	Ford, [19]	330-420°C Liquid phase
***n*C$_{16}$H$_{34}$**	61.2	1.5×10^{15}	Khorasheh and Gray, [20]	380-450°C 139 bar
***n*C$_{16}$H$_{34}$**	74	3.0×10^{19}	Jackson et al., [15]	300-370°C 150-600 bar
***n*C$_{25}$H$_{52}$**	68.2	6.1×10^{17}	Behar and Vandenbroucke, [14]	325-425°C 120-800 bar

Toluene	66.0	3.3×10^{13}	Domke et al., [47]	540-700°C 1 bar
Toluene	70.1	4.8×10^{14}	Clark and Price, [48]	?
1-methylnaphthalene	47.4	7.9×10^{9}	Leininger et al., [24]	380-450°C 100 bar
Trimethylbenzene	58.0	1.1×10^{12}	Fusetti et al., [31]	395-475°C 100 bar
Ethylbenzene	62.3	4.7×10^{13}	Domke et al., [47]	540-700°C 1 bar
Butylbenzene	65	3.0×10^{14}	Leigh and Szwarc, [49]	?
Butylbenzene	52.9	1.1×10^{12}	Freund and Olmstead, [50]	505-650°C
Butylbenzene	57	4.0×10^{17}	Yu and Eser, [51]	400-450°C 20-85 bar
Dodecylbenzene	53.3	1.3×10^{13}	Behar et al., [17]	325-425°C 140 bar
Pentadecylbenzene	55.5	1.1×10^{14}	Savage and Klein, [21]	375-450°C 1-9.7 bar
9-Methylphenanthrene	49.0	4.5×10^{10}	Behar et al., [13]	375-450°C 120 bar
Dibenzothiophene	59.0	1.9×10^{11}	Dartiguelongue et al., [18]	375-500°C 100 bar
2-Dodecyl-9,10-dihydrophenanthrene	54.5 ± 9.1	4.0×10^{13}	Savage and Baxter, [23]	375-450°C
Tetralin	58.0	3.5×10^{12}	Yu and Eser, 1998	425-475°C

				23-75 bar
2-Ethyltetralin	53.5	5.0×10^{12}	Savage and Klein, 1988	375-450°C
Propylcyclohexane	67.6	2.6×10^{16}	Widegren and Bruno, [53]	350-450°C 3500 bar
Butylcyclohexane	65.0	3.5×10^{15}	Yu and Eser, [54]	425-475°C 17-86 bar
Butylcyclohexane	69.0	6.7×10^{16}	Rakatoalimanana et al., [52]	300-425°C 100 bar

544 Table 4: Temperature-dependence of kinetic parameters of some hydrocarbons: influence on
545 conversion at 200°C.

546

	***n*C$_8$H$_{18}$**		***n*C$_{15}$H$_{32}$**	
	First-order law using A and Ea calculated at 400°C	First-order law using A and Ea calculated at 200°C	First-order law using A and Ea calculated at 400°C	First-order law using A and Ea calculated at 200°C
Conversion after 10 million years	91%	45%	93%	78%
	***n*C$_{25}$H$_{52}$**		**Toluene**	
	First-order law using A and Ea calculated at 400°C	First-order law using A and Ea calculated at 200°C	First-order law using A and Ea calculated at 400°C	First-order law using A and Ea calculated at 200°C
Conversion after 10 million years	91%	91%	49%	27%
	1-Methylnaphtalene		**Trimethylbenzene**	
	First-order law using A and Ea calculated at 400°C	First-order law using A and Ea calculated at 200°C	First-order law using A and Ea calculated at 400°C	First-order law using A and Ea calculated at 200°C
Conversion after 10 million years	100%	100%	96%	77%
	DB		**Tetralin**	
	First-order law using A and Ea calculated at 400°C	First-order law using A and Ea calculated at 200°C	First-order law using A and Ea calculated at 400°C	First-order law using A and Ea calculated at 200°C
Conversion after 100 million years	100% (98% after 1 million years)	100% (100% after 1 million years)	78%	99%
	MCH		**BCH**	
	First-order law using A and Ea calculated at	First-order law using A and Ea calculated at	First-order law using A and Ea calculated at	First-order law using A and Ea calculated at

	400°C	200°C	400°C	200°C
Conversion after 100 million years	89%	63%	97%	87%

547

548

549 **Figure captions**

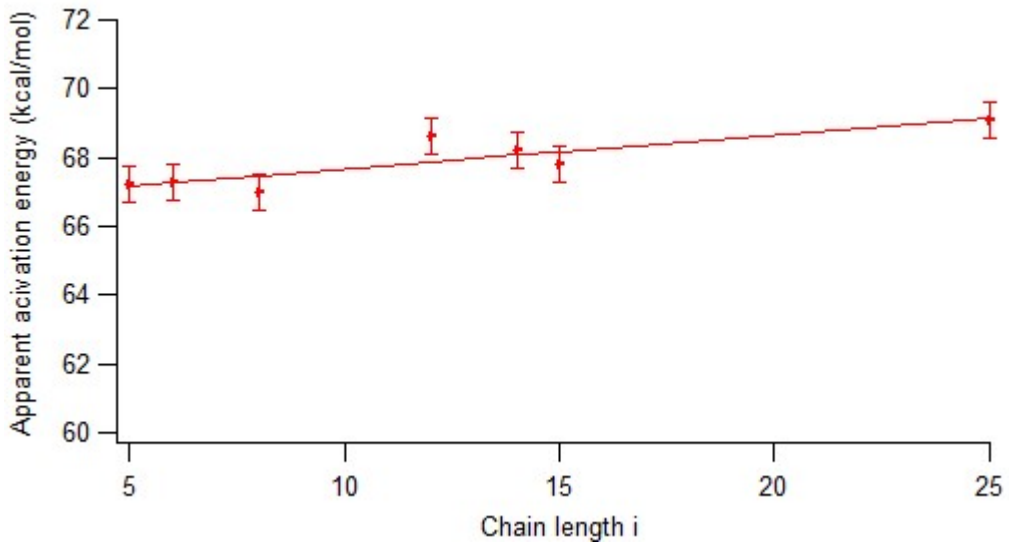

550

551 Figure 1: Apparent activation energy computed at 400°C as a function of the chain length *i*
552 (linear regression: E_a *(kcal/mol)* = *0.10*×*i* + *66.7*).

553

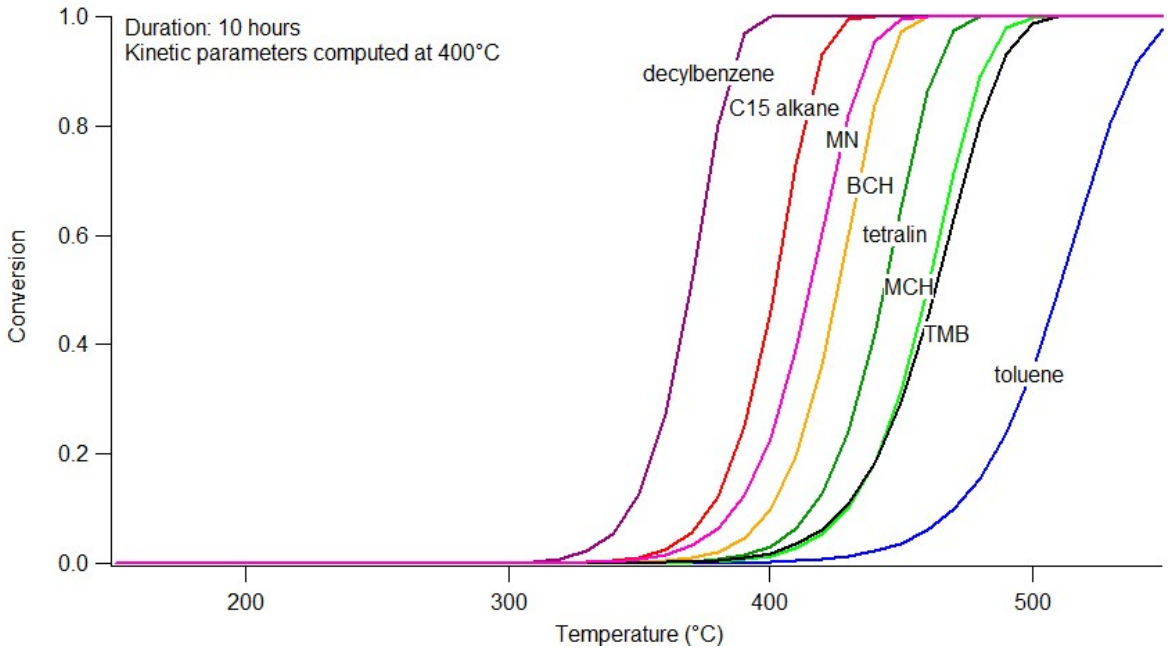

554

555

556

557

558

Figure 2: Relative stability of the hydrocarbons determined by using the apparent kinetic parameters calculated at 400°C (pyrolysis duration set to 10 h).

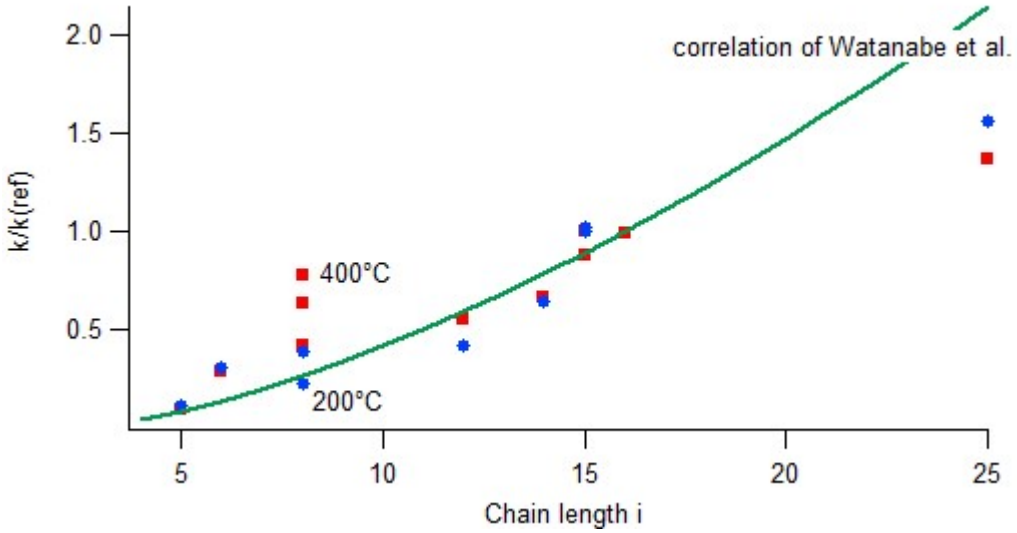

Figure 3: Comparison of the normalized rate constants [26, 29, 30, 33] (C_{15} as the reference compound) as a function of the chain length to the correlation of Watanabe et al. [55] (square markers: 400°C and circle markers: 200°C).

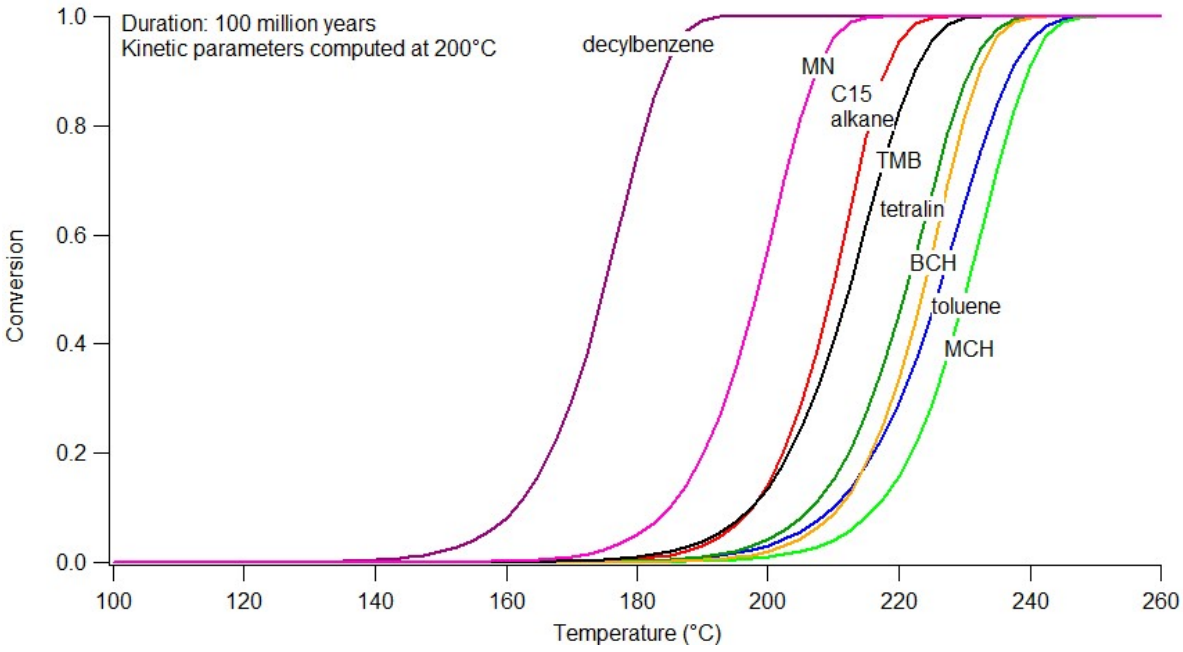

Figure 4: Relative stability of the hydrocarbons determined by using the apparent kinetic parameters calculated at 200°C (pyrolysis duration set to 100 million years).

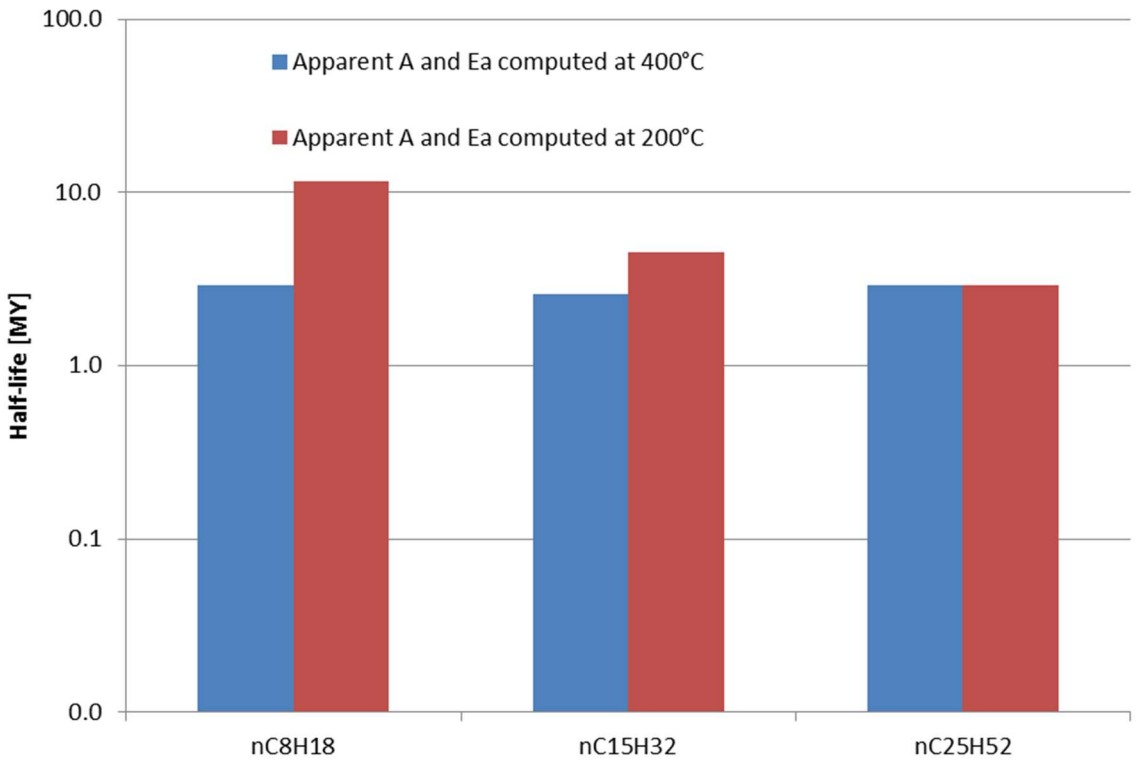

571

572 Figure 5: Temperature-dependence of kinetic parameters of some alkanes: influence on half-
573 life at 200°C.

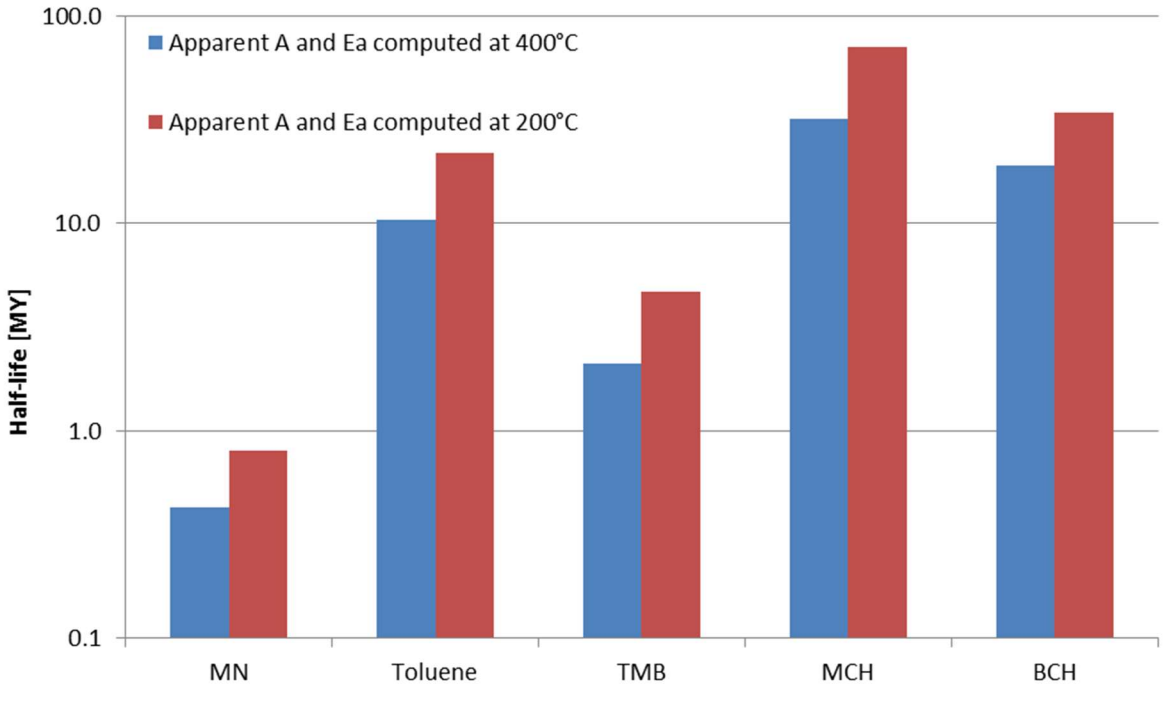

574

575 Figure 6: Temperature-dependence of kinetic parameters of methylaromatics and naphthenes:
576 influence on half-life at 200°C.

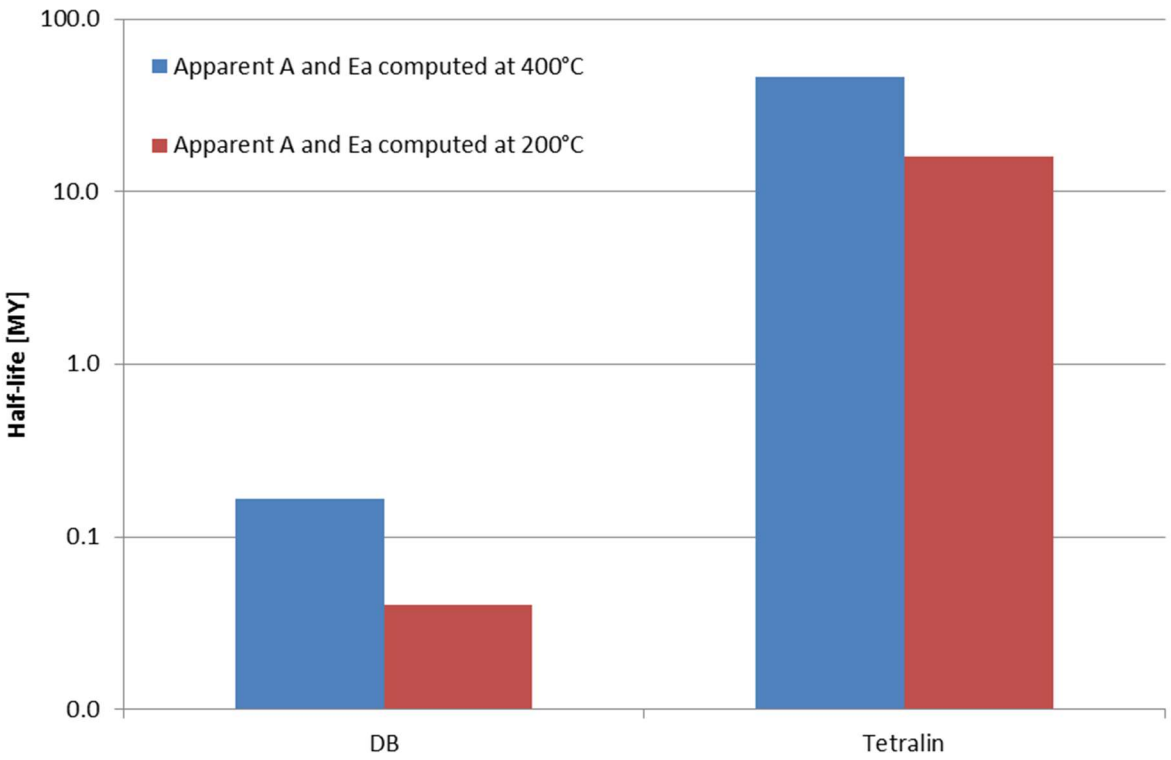

577

578 Figure 7: Temperature-dependence of kinetic parameters of decylbenzene and tetralin:
579 influence on half-life at 200°C.

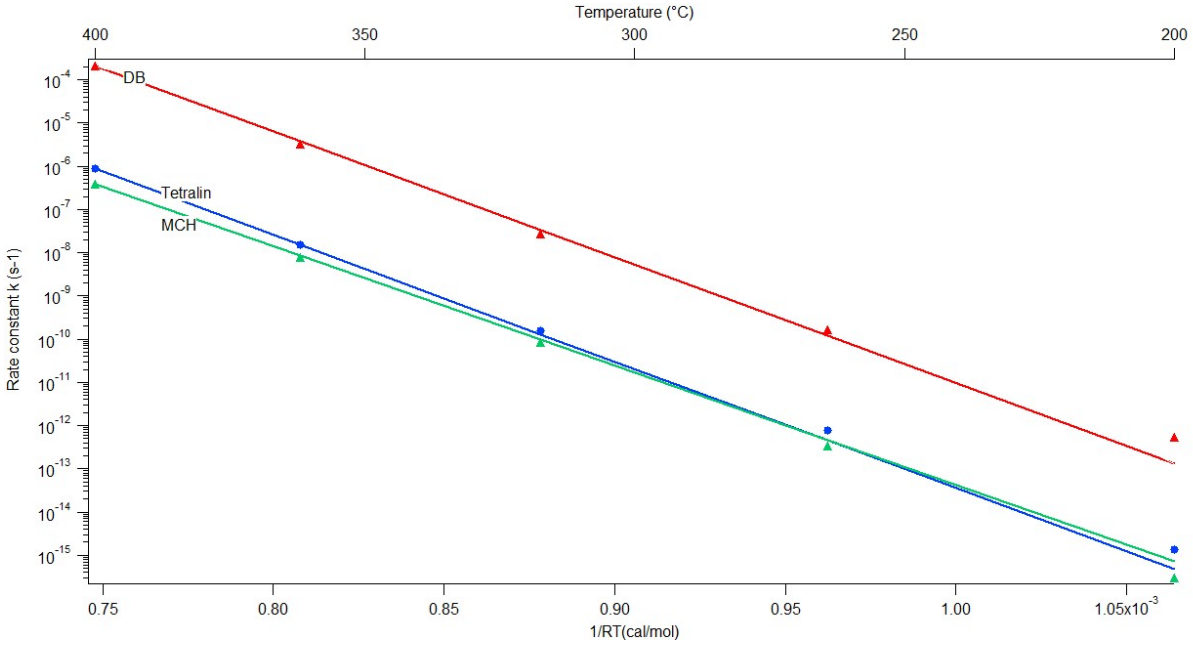

580

581 Figure 8: Computed evolution of the rate constants (decylbenzene, methylcyclohexane and
582 tetralin) as a function of temperature compared with the extrapolation of the Arrhenius law
583 from 400°C.

584

585

586

587

588

589